HHS Public Access

Author manuscript

DNA Repair (Amst). Author manuscript; available in PMC 2022 December 01.

Published in final edited form as:

DNA Repair (Amst). 2021 December ; 108: 103227. doi:10.1016/j.dnarep.2021.103227.

XRCC3 loss leads to midgestational embryonic lethality in mice

Rohit Prakash[1,2], **Laina Freyer**[1,3], **Néstor Saiz**[1,4], **Svetlana Gavrilov**[1,5], **Raymond Wang**[1], **Peter Romanienko**[1,6], **Elizabeth Lacy**[1], **Anna-Katerina Hadjantonakis**[1], **Maria Jasin**[1,+]

[1]Developmental Biology Program, Memorial Sloan Kettering Cancer Center, New York, NY

[2]Regeneron Pharmaceuticals, Tarrytown, New York, NY

[3]Institut Pasteur, Paris, France

[4]Rockefeller University Press, New York, NY

[5]Bristol-Myers Squibb, New York, NY

[6]Rutgers-Cancer Institute of New Jersey, New Brunswick, NJ

Abstract

RAD51 paralogs are key components of the homologous recombination (HR) machinery. Mouse mutants have been reported for four of the canonical RAD51 paralogs, and each of these mutants exhibits embryonic lethality, although at different gestational stages. However, the phenotype of mice deficient in the fifth RAD51 paralog, XRCC3, has not been reported. Here we report that *Xrcc3* knockout mice exhibit midgestational lethality, with mild phenotypes beginning at about E8.25 but severe developmental abnormalities evident by E9.0–9.5. The most obvious phenotypes are small size and a failure of the embryo to turn to a fetal position. A knockin mutation at a key ATPase residue in the Walker A box results in embryonic lethality at a similar stage. Death of knockout mice can be delayed a few days for some embryos by homozygous or heterozygous *Trp53* mutation, in keeping with an important role for XRCC3 in promoting genome integrity. Given that XRCC3 is a unique member of one of two RAD51 paralog complexes with RAD51C, these results demonstrate that both RAD51 paralog complexes are required for mouse development.

Keywords

XRCC3; RAD51 paralog; mouse embryogenesis; ATPase mutant; Walker A box mutation

[+]Corresponding author: m-jasin@ski.mskcc.org, 430 East 67 Street, Memorial Sloan Kettering Cancer Center, New York, NY 10065.

Author contributions

R.P. and M.J. conceived the project. R.P., L.F., N.S., S.G., R.W., and P.J.R. designed and conducted experiments. E.L., A.K.H. and M.J. provided supervision. R.P. and M.J. wrote the manuscript, with input from E.L. and A.K.H.

Conflict of Interest statement

The authors declare that there are no conflicts of interest.

1. Introduction

Homologous recombination (HR) is a crucial DNA repair mechanism in mammalian cells [1]. The central step in HR pathways is strand exchange, in which single-stranded DNA (ssDNA) invades a homologous duplex DNA, driven by the RAD51/RecA family of ATPases. RAD51 performs this function in mammalian cells, forming a nucleoprotein filament with ssDNA which performs the homology search and catalyzes strand exchange [2]. In vivo RAD51 requires the assistance of numerous factors to nucleate RAD51 filament formation on ssDNA and/or promote stable filament assembly [2–4]. Among the factors involved in this process are RAD51 paralogs, which have limited homology to RAD51 in the ATPase domain. Biochemical studies have suggested that these proteins act as chaperones to promote the assembly of RAD51 filaments on ssDNA [5] and/or remodel the RAD51 nucleoprotein filament to promote the recognition of a homologous duplex [6]. In mammalian cells, there are five canonical RAD51 paralogs that were discovered through partial sequence identity with RAD51 (RAD51B, [7]; RAD51C, [8]; RAD51D, [9]) or complementation of radiation-sensitive Chinese hamster cell mutants (XRCC2, [10]; XRCC3, [11]). Biochemically, the paralogs have been shown to form two complexes, RAD51C-XRCC3 and RAD51B-RAD51C-RAD51D-XRCC2 [12]. More recently, an additional RAD51 paralog, SWSAP1, has been identified with more limited roles in HR [13].

As with *Rad51*, null mutations in *Rad51b, Rad51c, Rad51d,* or *Xrcc2* result in embryonic lethality in mice [3]. Mutants die at somewhat different embryonic (E) stages, although the exact timing of death may be influenced by genetic background or possibly the particular mutation being examined. *Rad51* mutant embryos have been reported to die before or shortly after implantation, depending on the study [14, 15]. *Rad51b* and *Rad51c* mutant embryos show abnormalities during early stages of postimplantation development (E5.5) [16, 17], while *Rad51d* mutant embryos display abnormalities a few days later at gastrulation (E7.5) [18]. *Xrcc2* embryos have been reported to develop normally until E8.5, with variability in subsequent survival; a few mutant mice have even been born, but they are not viable [19]. However, *Xrcc2* mutant mice on a C57BL/6 background succumb before late embryogenesis [20]. By contrast, mutation of the noncanonical RAD51 paralog *Swsap1* does not affect embryonic or post-natal viability, although mice are infertile [21].

Surprisingly, despite its identification more than two decades ago as a key HR factor [22], the phenotype of *Xrcc3* knockout in mice has not been reported. We sought to rectify this gap in our knowledge and now report midgestational embryonic lethality associated with loss of *Xrcc3*.

2. Materials and Methods

2.1 Mouse care

The care and use of mice in this study were in accordance with a protocol approved by the Institutional Animal Care and Use Committee (IACUC) at Memorial Sloan Kettering Cancer Center (MSKCC). Mice were housed under federal regulations and policies governed by the

Animal Welfare Act (AWA) and the Health Research Extension Act of 1985 in the Research Animal Resource Center (RARC) at MSKCC and was overseen by IACUC.

2.2 Generation and genotyping of *Xrcc3* mice and embryos

TALE nucleases (TALENs) were generated [23] and injected into fertilized mouse eggs [24]. *Xrcc3* null mice were generated using TALENs directed towards the first coding exon (exon 2), beginning at the translational start site. For *Xrcc3* KA mice, TALENs were designed to cleave in exon 4. To generate the KA knockin mutation, a plasmid containing 2 kb of homology to exon 4 and surrounding sequences was modified to contain the K113A mutation and two silent mutations nearby to create an MfeI restriction enzyme site and co-injected at 10 ng/μl with TALEN mRNA. The 2 kb fragment was initially generated by PCR of genomic DNA in two steps using primers:

Xrcc3G AGGTCGACGGTATCGATACAGCCACGATGTGCAGTGCCTG

Xrcc3H GCGCCAatTGGGTGGCTCCTGCTGAGCTGCAGCCAGCCAGGC

Xrcc3J CAGGAGCCACCCAatTGGCGCTACAGCTCTGCCTGGCTGTGC

Xrcc3K GGGCTGGACGAATTCGATCTGGCCTCCAGCCTGCATTGATC

Genotyping of *Xrcc3* null mice was done using PCR primers *Xrcc3*-C: 5′-ACACCTAACCACACTTTGGCTTCG-3′, and *Xrcc3*-D: 5′-GAGAGTGCAGCTTGTTTTGCCCAC-3′ under the following PCR conditions: 94 °C, 3 min; 35 cycles of 94 °C, 30 s; 55 °C, 30 s and 65 °C 30 s; and a final extension of 72 °C, 5 min. Initially, mutations were characterized by DNA sequencing. For the *Δ11* and *Δ22* alleles, subsequent genotyping was performed by digesting the PCR product with Sau96I and running on a 1.5% agarose gel. The wild-type product prior to digestion is 268 bp, but is cleaved by Sau96I to products of 165 and 103 bp. The PCR products from the *Δ11* and *Δ22* alleles are smaller by 11 and 22 bp, respectively, and are not cleaved by Sau96I.

Genotyping of the KA knockin mice was done using PCR primers: *Xrcc3*-KA-E: 5′-GCTAGACCGCTGACACAGCCTG-3′, and *Xrcc3*-KA-F: 5′-AAACCACTCAAGAGATAGCCACTG-3′ under the following PCR conditions: 94 °C, 3 min; 35 cycles of 94 °C, 30 s; 55 °C, 30 s and 65 °C 30 s; and a final extension of 72 °C, 5 min. The PCR product was digested with MfeI and run on a 1.5% agarose gel. The wild-type and KA products are 372 bp. After digestion with MfeI, the KA PCR product, but not the wild-type PCR product, is cleaved to fragments of 188 and 184 bp.

The *Trp53* allele has been previously described [25] and was genotyped with PCR primers x7: 5’-TATACTCAGAGCCGGCCT-3′, x6.5: 5’-ACAGCGTGGTGGTACCTTAT-3′, and p53 neo: 5’-TCCTCGTGCTTTACGGTATC-3′.

Mice with knockout and knockin alleles were backcrossed onto a C57BL/6N background for at least 3 or 4 generations. For timed matings, heterozygous mice were intercrossed, and the day of vaginal plug was considered to be embryonic day E0.5. The stage of embryonic development was confirmed upon dissection by morphological landmarks or counting the

numbers of somite pairs when possible. The yolk sac was used for genotyping embryos, except at E3.5.

Xrcc3^{tm1b} mice generated by KOMP [26] and analyzed by the IMPC were on a C57BL/6NJ background (https://www.mousephenotype.org/data/genes/MGI:1921585). In the IMPC E12.5 viability screen, no mutants were obtained among 23 heterozygous and 7 wild-type embryos. For our analysis, we crossed a heterozygous male on a C57BL/6N background to FVB females to obtain heterozygous males and females. F1 intercross litters dissected at both ~E8.5 and E9.0 were subsequently analyzed.

2.3 In-situ hybridization and *LacZ* analysis

Embryos (E8.25-E9.5) were fixed in 4% paraformaldehyde overnight followed by dehydration in a methanol/PBT (0.1% Tween-20 in PBS) series. Hybridization buffer was composed of 50% formamide, 1% Boehringer block, 5X SSC pH 7.0, 1 mg/mL Torula RNA, 100 μg/mL Heparin, 0.5% Tween-20, 1 mg/mL CHAPS (3-((3-cholamidopropyl) dimethylammonio)-1-propanesulfonate), and 5 mM EDTA pH 8.0. Embryos were blocked in antibody buffer composed of PBS, 1% Boehringer block, 10% heat-inactivated fetal bovine serum, and 0.1% Tween-20. Riboprobes were detected using anti-digoxigenin-AP, Fab fragments (Roche 11093274910, 1:10,000), and BM purple (Roche 11442074001).

The following digoxigenin-labeled riboprobes were synthesized by RNA polymerases (Roche) using existing plasmids that were linearized by restriction enzyme digest and are available from the Hadjantonakis lab: *Brachyury* (linearized with BamHI and transcribed by T7 polymerase); *Meox1 (Mox-1)* (linearized with Pst1 and transcribed by T3 polymerase); *Fgf8* (linearized with Pst1 and transcribed by T7 polymerase); *Nkx2.5* (linearized with XbaI and transcribed by T7 polymerase).

LacZ expression was measured using β-galactosidase activity using Salmon-gal (6-chloro-3-indolyl-β-D-galactopyranoside) (Lab Scientific, catalog number X668) in combination with tetrazolium salts, as previously described [27].

2.4 Statistical analysis

Statistical analyses were performed using a two-tailed Student's *t*-test. Error bars, mean ± s.d. $*P \leq 0.05$; $***P \leq 0.001$.

3. Results

3.1 *Xrcc3* mutant mice are not viable

To disrupt *Xrcc3*, gene editing was performed in mouse zygotes using TALENs directed to exon 2 at a site just downstream of the start codon. Four small deletion alleles (*Δ2, Δ7, Δ11, Δ22*) were obtained in founder mice, each of which disrupted the *Xrcc3* reading frame (Fig. 1A). Heterozygous progeny obtained from founders for each allele were interbred and, despite extensive breeding, no homozygous mutant pups were obtained (Fig. 1B), indicating that *Xrcc3* mutant mice are not viable.

3.2 Mid-gestational embryonic lethality with loss of *Xrcc3*

To determine the latest embryonic stage to which *Xrcc3* mutant embryos develop, timed matings were performed using heterozygous parents. We typically used the *Δ11* allele, which could be genotyped by loss of a Sau96I restriction site (Fig. 1A,C). *Xrcc3* mutant embryos were not obtained at E13.5 or E12.5 but were present at E9.5 (Fig. 1D), although at this stage they exhibited severe developmental abnormalities. During normal embryogenesis, E9.5 mouse embryos have undergone axial rotation (or 'turning') into a fetal position, a process that begins during the 6–8 somite stage and is usually completed by the 14–16 somite stage, leading to the complete encasement of the embryo in extraembryonic membranes [28]. However, the vast majority of *Xrcc3* mutant embryos (16/17) remained in the U-shaped lordotic position (Fig. 1E). Therefore, mutant embryos at E9.5 were more akin morphologically to E8.25 embryos (Fig. 1F). Moreover, even at E8.25, *Xrcc3* mutant embryos were typically developmentally delayed. Embryos were often smaller, with a reduced number of somites compared to heterozygous and wild-type littermates (Fig. 1G).

In addition to the gene edited *Xrcc3* alleles, we examined $Xrcc3^{tm1b}$, an exon 2 deletion generated by the Knockout Mouse Project (KOMP) and found by the International Mouse Phenotyping Consortium (IMPC) to show completely penetrant embryonic lethality prior to E12.5 (www.mousephenotype.org). We examined 11 litters recovered from $Xrcc3^{tm1b/+}$ intercross matings at E8.5, E9.0, or E10.5. Of the 89 genotyped embryos, 17 were $Xrcc3^{tm1b/tm1b}$ homozygotes (19.1%), 44 were $Xrcc3^{tm1b/+}$ heterozygotes (49.4%), and 28 wild type (31.5%). The 5 mutants recovered at E10.5 were dead and degrading, while the 12 mutants recovered at E8.5-E9.0 displayed a phenotype similar to that observed for the $Xrcc3^{\Delta 11/\Delta 11}$ mutants: arrest at the 6–8 somite stage prior to axial rotation (Fig. S1A).

To further characterize the mutant embryos, in situ hybridization was performed with a set of markers. At E9.25, *Brachyury* labels the tail bud, the last active region of the primitive streak [29], while *Meox1* (*Mox-1*) serves as a marker for paraxial mesoderm, both before and after somite formation [30]. In *Xrcc3* mutant embryos, both markers were present, suggesting that the absence of somites in some mutant embryos does not reflect a lack of paraxial mesoderm (Fig. 1E). At E8.25, *Fgf8* labels the midbrain/hindbrain boundary, the anterior neural ridge, the branchial arches, and the posterior end of the primitive streak [31]. *Xrcc3* mutants appropriately expressed *Fgf8* in the posterior streak and branchial arches. However, embryos with the *Δ11* allele (5 total) lacked *Fgf8* expression at the anterior neural ridge and midbrain/hindbrain boundary; this finding indicates that the small head region observed in $Xrcc3^{\Delta 11/\Delta 11}$ embryos at E8.25 and E9.25 (Fig.1E, F) and in $Xrcc3^{tm1b/tm1b}$ embryos at E9.0 (Fig. S1A) likely reflects impaired mid-brain development. Mutants with the *Δ22* allele fail to turn to a fetal position, comparable to mutants with the *tm1b* or *Δ11* allele; yet the detection of *Fgf8* expression at the anterior neural ridge and midbrain/hindbrain boundary of E8.25 $Xrcc3^{\Delta 22/\Delta 22}$ embryos (1 total, Fig. 1F), suggests that the *Δ11* and *tm1b* alleles may be slightly more severe. At E8.25 *Nkx2.5,* a marker for cardiac progenitors [32], labels the developing heart of both control and *Xrcc3* mutants at (Fig.1F). However, the proportionally large hearts present in *Xrcc3* mutants at E9–9.25 (Fig. 1E, *Δ11;* Fig. S1A, *tm1b*), indicate that the progenitors undergo aberrant morphogenesis producing cardiac hypertrophy and edema from impaired blood flow.

We also examined embryos at earlier embryonic stages. At gastrulation (E7.5 and E6.5), *Xrcc3* mutant embryos were recovered at Mendelian ratios and appeared grossly normal (Figs. 1D,H,I). Blastocysts were also obtained at E3.5 to attempt embryonic stem (ES) cell line derivation. Although *Xrcc3* mutant lines could be derived, they grew slowly and were not further characterized.

In summary, mouse embryos lacking functional *Xrcc3* develop normally through the early post implantation stages: They establish an anterior-posterior axis, gastrulate to generate the three definitive germ layers plus extraembryonic mesoderm, and initiate formation of the heart. Between the late headfold stage and the onset of early somitogenesis profound global defects become evident with developmental arrest.

3.3 *Xrcc3* mutant embryos can develop further with *Trp53* mutation

Loss of p53 has been shown to prolong survival of embryos with mutations in HR genes, in keeping with suppression of the response to DNA damage associated with HR deficiency [3]. In the most extreme case, mutation of *Trp53* rescues the late embryonic lethality associated with loss of *Xrcc2*, another RAD51 paralog, giving rise to live borne mice, although they rapidly succumb to tumors [33]. Therefore, we sought to determine whether *Trp53* mutation would also rescue *Xrcc3* mutant mice. At weaning, $Xrcc3^{\Delta 11/\Delta 11}$ mice with homozygous or heterozygous *Trp53* mutation were not observed (Fig. 2A), indicating thatcomplete or partial loss of *Trp53* is not sufficient to rescue the embryonic lethality associated with loss of XRCC3. However, timed matings demonstrated that *Trp53* mutation could have a dramatic effect on some embryos. At E9.5, of six mutant embryos with *Trp53* heterozygosity, three had turned into the fetal position and 1 other was also more advanced, although another was more similar to an E8.25 embryo. (Damage during dissection prevented assessing the sixth mutant.) In addition, all three E9.5 $Xrcc3^{\Delta 11/\Delta 11}$ mutant embryos homozygous for the *Trp53* mutation advanced through turning (Fig. 2B,C; Fig. S1B). Moreover, at E12.5 when $Xrcc3^{\Delta 11/\Delta 11}$ mutant embryos are not observed (Fig. 1D), mice heterozygous (2 embryos) and homozygous (1 embryo) for the *Trp53* mutation were observed, and the latter appeared relatively normal (Fig. 2D,E). The phenotypic variability observed with *Trp53* mutation is similar to that observed for other HR mutant embryos.

3.4 *Xrcc3* K113A mutation in the Walker A box also leads to embryonic lethality

The Walker A box (GxxxxGKT) is a critical motif for ATP binding/hydrolysis in RAD51 and related proteins and has previously been shown to be important for XRCC3 function: a K113A mutation within this box (GxxxxGAT) reduces HR levels in *Xrcc3* mutant hamster cells, although HR is not abolished (~20–25% activity relative to wild type) [34]. However, the residual amount of HR activity observed with the K113A mutant in cultured cells led us to ask whether the cognate mouse mutant would survive longer during embryogenesis or even be viable.

To that end, we knocked-in the K113A mutation within exon 4 in mouse zygotes using TALENs and a double-stranded DNA donor that additionally brought in two silent polymorphisms, which create an MfeI restriction site to simplify genotyping (Fig. 2F). With

this approach, we obtained the K113A (*KA*) knockin mutation as well as two frameshift alleles through NHEJ (*Δ8, Δins*). Heterozygous breeding indicated that homozygous *KA* mutant mice were not viable (Fig. 2G). Mice homozygous for either frameshift allele were also inviable, in line with the truncations within exon 2.

Timed matings were then performed to determine at what stage the mice became compromised. Although at E9.5, $Xrcc3^{KA/KA}$ embryos could be obtained (Fig. 2H,I), they all appeared small and delayed in development (Fig. 2J, Fig. S1C). Similarly, mutant embryos could be obtained at E8.25, but they were also runted and possibly further delayed and/or morphologically aberrant compared with the null embryos (5/7 embryos) (Fig. 2I, Fig. S1D). By contrast, heterozygous embryos were infrequently observed to be delayed (3/21 embryos), and heterozygous adults were recovered at Mendelian ratios and were fertile.

Discussion

Here we report midgestational lethality associated with XRCC3 loss. Global defects are observed between E8.25 and E9.5, a critical transition phase during mouse development when the embryo rotates along its longitudinal axis. What drives axial rotation remains unclear, making it infeasible to ascertain whether any one specific defect blocks this transition or whether the multiple observed defects, including reduced size, conspire to obstruck axial rotation. Just prior to this stage, at E6.5-to-E7.5, the embryo undergoes a period of particularly rapid proliferation, when epiblast cell cycles can be as short as 2.2 h [35]. Consequently the requirement for XRCC3, and other HR genes, during these embryonic stages may reflect their essential role in resolving replication stress and maintaining genomic integrity [36–38]. The phenotype of the *Trp53*-rescued $Xrcc3^{\Delta 11/\Delta 11}$ mutants indicates that loss of XRCC3 does not perturb lineage specification and patterning and, moreover, suggests that loss of cell number underlies the observed morphological defects.

While the other four canonical RAD51 paralogs form the RAD51B-RAD51C-RAD51D-XRCC2 (BCDX2) complex, XRCC3 is the unique member of a distinct complex with RAD51C. Thus, XRCC3, and by inference the RAD51C-XRCC3 complex, has an essential, non-redundant role with the four member BCDX2 complex during mouse embryogenesis. Why two RAD51 paralog complexes are required is unclear and needs further biochemical and cellular characterization. Early work had suggested that RAD51C-XRCC3 has a distinct, later role in HR, in particular, in the resolution of recombination intermediates [39]. However, analysis of an isogenic series of RAD51 paralog knockout human cells has demonstrated a clear requirement for XRCC3 in an early step in HR like other RAD51 paralogs, namely in the formation of DNA damage induced RAD51 focus formation [40]. Analysis of this series indicates that loss of XRCC3 does not affect RAD51C stability, implying that XRCC3 has an intrinsic role in HR.

The delay in the embryonic lethality associated with XRCC3 loss by either homozygous or heterozygous *Trp53* mutation is consistent with the inability of *Xrcc3* mutants to properly repair DNA damage arising during normal development, as has been seen in other paralog

mutants [3]. Lethality with the *KA* knockin mutation indicates a requirement for ATP binding/hydrolysis in its function. The more severe phenotype observed with some of the knockin embryos suggests the mutant protein may be interfering with the activity of another protein, potentially its interacting protein RAD51C.

Among the other RAD51 paralog mutants, the one closest in phenotype is *Rad51d*, in which most embryos are grossly retarded and fail to turn, such that no viable embryos are found by E11.5 [18]. *Rad51c* mutation has been reported to be more severe than either *Xrcc3* or *Rad51d* [17], possibly because RAD51C is a critical member of both RAD51 paralog complexes. Interestingly, however, *Rad51b* mutant embryos are also more severe than *Xrcc3* embryos [16] while *Xrcc2* embryos are less severe [20]. Thus, the three unique members of the BCDX2 complex, RAD51B, RAD51C, and XRCC2, are not identically required during mouse development, possibly due to the degree of HR deficiency with mutation of each and the stochastic accumulation of DNA damage. In human cells, four of the five RAD51 paralogs, including XRCC3, are essential for the proliferation of the non-transformed cell line MCF10A; the one exception is RAD51B [40], suggesting that there are differences between the absolute requirements of these factors between mouse and human.

Supplementary Material

Refer to Web version on PubMed Central for supplementary material.

Acknowledgements

The authors thank Alex Joyner for discussions. Funding from the National Institutes of Health, including the Cancer Center Core Grant P30CA008748, 5R01 HD086478 (E.L.), R01HD094868 and DK127821 (A.-K. H.), and R35CA253174 (M.J.).

References

[1]. Liang F, Han M, Romanienko PJ, Jasin M, Homology-directed repair is a major double-strand break repair pathway in mammalian cells, Proc Natl Acad Sci U S A 95 (1998) 5172–5177. [PubMed: 9560248]

[2]. Bell JC, Kowalczykowski SC, Mechanics and Single-Molecule Interrogation of DNA Recombination, Annu Rev Biochem 85 (2016) 193–226. [PubMed: 27088880]

[3]. Prakash R, Zhang Y, Feng W, Jasin M, Homologous recombination and human health: the roles of BRCA1, BRCA2, and associated proteins, Cold Spring Harb Perspect Biol 7 (2015) a016600. [PubMed: 25833843]

[4]. Zhao W, Wiese C, Kwon Y, Hromas R, Sung P, The BRCA Tumor Suppressor Network in Chromosome Damage Repair by Homologous Recombination, Annu Rev Biochem 88 (2019) 221–245. [PubMed: 30917004]

[5]. Roy U, Kwon Y, Marie L, Symington L, Sung P, Lisby M, Greene EC, The Rad51 paralog complex Rad55-Rad57 acts as a molecular chaperone during homologous recombination, Mol Cell 81 (2021) 1043–1057 e1048. [PubMed: 33421364]

[6]. Taylor MRG, Spirek M, Chaurasiya KR, Ward JD, Carzaniga R, Yu X, Egelman EH, Collinson LM, Rueda D, Krejci L, Boulton SJ, Rad51 Paralogs Remodel Pre-synaptic Rad51 Filaments to Stimulate Homologous Recombination, Cell 162 (2015) 271–286. [PubMed: 26186187]

[7]. Albala JS, Thelen MP, Prange C, Fan W, Christensen M, Thompson LH, Lennon GG, Identification of a novel human RAD51 homolog, RAD51B, Genomics 46 (1997) 476–479. [PubMed: 9441753]

[8]. Dosanjh MK, Collins DW, Fan W, Lennon GG, Albala JS, Shen Z, Schild D, Isolation and characterization of RAD51C, a new human member of the RAD51 family of related genes, Nucleic Acids Res 26 (1998) 1179–1184. [PubMed: 9469824]

[9]. Pittman DL, Weinberg LR, Schimenti JC, Identification, characterization, and genetic mapping of Rad51d, a new mouse and human RAD51/RecA-related gene, Genomics 49 (1998) 103–111. [PubMed: 9570954]

[10]. Cartwright R, Tambini CE, Simpson PJ, Thacker J, The XRCC2 DNA repair gene from human and mouse encodes a novel member of the recA/RAD51 family, Nucleic Acids Res 26 (1998) 3084–3089. [PubMed: 9628903]

[11]. Tebbs RS, Zhao Y, Tucker JD, Scheerer JB, Siciliano MJ, Hwang M, Liu N, Legerski RJ, Thompson LH, Correction of chromosomal instability and sensitivity to diverse mutagens by a cloned cDNA of the XRCC3 DNA repair gene, Proc Natl Acad Sci U S A 92 (1995) 6354–6358. [PubMed: 7603995]

[12]. Masson JY, Tarsounas MC, Stasiak AZ, Stasiak A, Shah R, McIlwraith MJ, Benson FE, West SC, Identification and purification of two distinct complexes containing the five RAD51 paralogs, Genes Dev 15 (2001) 3296–3307. [PubMed: 11751635]

[13]. Liu T, Wan L, Wu Y, Chen J, Huang J, hSWS1.SWSAP1 is an evolutionarily conserved complex required for efficient homologous recombination repair, J Biol Chem 286 (2011) 41758–41766. [PubMed: 21965664]

[14]. Lim DS, Hasty P, A mutation in mouse rad51 results in an early embryonic lethal that is suppressed by a mutation in p53, Mol Cell Biol 16 (1996) 7133–7143. [PubMed: 8943369]

[15]. Tsuzuki T, Fujii Y, Sakumi K, Tominaga Y, Nakao K, Sekiguchi M, Matsushiro A, Yoshimura Y, MoritaT, Targeted disruption of the Rad51 gene leads to lethality in embryonic mice, Proc Natl Acad Sci U S A 93 (1996) 6236–6240. [PubMed: 8692798]

[16]. Shu Z, Smith S, Wang L, Rice MC, Kmiec EB, Disruption of muREC2/RAD51L1 in mice results in early embryonic lethality which can Be partially rescued in a p53(−/−) background, Mol Cell Biol 19 (1999) 8686–8693. [PubMed: 10567591]

[17]. Kuznetsov SG, Haines DC, Martin BK, Sharan SK, Loss of Rad51c leads to embryonic lethality and modulation of Trp53-dependent tumorigenesis in mice, Cancer Res 69 (2009) 863–872. [PubMed: 19155299]

[18]. Pittman DL, Schimenti JC, Midgestation lethality in mice deficient for the RecA-related gene, Rad51d/Rad51l3, Genesis 26 (2000) 167–173. [PubMed: 10705376]

[19]. Deans B, Griffin CS, Maconochie M, Thacker J, Xrcc2 is required for genetic stability, embryonic neurogenesis and viability in mice, EMBO J 19 (2000) 6675–6685. [PubMed: 11118202]

[20]. Adam J, Deans B, Thacker J, A role for Xrcc2 in the early stages of mouse development, DNA Repair (Amst) 6 (2007) 224–234. [PubMed: 17116431]

[21]. Abreu CM, Prakash R, Romanienko PJ, Roig I, Keeney S, Jasin M, Shu complex SWS1-SWSAP1 promotes early steps in mouse meiotic recombination, Nat Commun 9 (2018) 3961. [PubMed: 30305635]

[22]. Pierce AJ, Johnson RD, Thompson LH, Jasin M, XRCC3 promotes homology-directed repair of DNA damage in mammalian cells, Genes Dev 13 (1999) 2633–2638. [PubMed: 10541549]

[23]. Cermak T, Doyle EL, Christian M, Wang L, Zhang Y, Schmidt C, Baller JA, Somia NV, Bogdanove AJ, Voytas DF, Efficient design and assembly of custom TALEN and other TAL effector-based constructs for DNA targeting, Nucleic Acids Res 39 (2011) e82. [PubMed: 21493687]

[24]. Wefers B, Ortiz O, Wurst W, Kuhn R, Generation of targeted mouse mutants by embryo microinjection of TALENs, Methods 69 (2014) 94–101. [PubMed: 24418396]

[25]. Jacks T, Remington L, Williams BO, Schmitt EM, Halachmi S, Bronson RT, Weinberg RA, Tumor spectrum analysis in p53-mutant mice, Curr Biol 4 (1994) 1–7. [PubMed: 7922305]

[26]. Dickinson ME, Flenniken AM, Ji X, Teboul L, Wong MD, White JK, Meehan TF, Weninger WJ, Westerberg H, Adissu H, Baker CN, Bower L, Brown JM, Caddle LB, Chiani F, Clary D, Cleak J, Daly MJ, Denegre JM, Doe B, Dolan ME, Edie SM, Fuchs H, Gailus-Durner V, Galli A, Gambadoro A, Gallegos J, Guo S, Horner NR, Hsu CW, Johnson SJ, Kalaga S, Keith LC,

Lanoue L, Lawson TN, Lek M, Mark M, Marschall S, Mason J, McElwee ML, Newbigging S, Nutter LM, Peterson KA, Ramirez-Solis R, Rowland DJ, Ryder E, Samocha KE, Seavitt JR, Selloum M, Szoke-Kovacs Z, Tamura M, Trainor AG, Tudose I, Wakana S, Warren J, Wendling O, West DB, Wong L, Yoshiki A, C. International Mouse Phenotyping, Jackson L, I.C.d.l.S. Infrastructure Nationale Phenomin, Charles River L, Harwell MRC, Toronto Centre for P, Wellcome Trust Sanger I, Center RB, MacArthur DG, Tocchini-Valentini GP, Gao X, Flicek P, Bradley A, Skarnes WC, Justice MJ, Parkinson HE, Moore M, Wells S, Braun RE, Svenson KL, de Angelis MH, Herault Y, Mohun T, Mallon AM, Henkelman RM, Brown SD, Adams DJ, Lloyd KC, McKerlie C, Beaudet AL, Bucan M, Murray SA, High-throughput discovery of novel developmental phenotypes, Nature 537 (2016) 508–514. [PubMed: 27626380]

[27]. Sundararajan S, Wakamiya M, Behringer RR, Rivera-Perez JA, A fast and sensitive alternative for beta-galactosidase detection in mouse embryos, Development 139 (2012) 4484–4490. [PubMed: 23132248]

[28]. Kaufman MH, The Atlas of Mouse Development, Academic Press, London, 1992.

[29]. Herrmann BG, Expression pattern of the Brachyury gene in whole-mount TWis/TWis mutant embryos, Development 113 (1991) 913–917. [PubMed: 1821859]

[30]. Candia AF, Hu J, Crosby J, Lalley PA, Noden D, Nadeau JH, Wright CV, Mox-1 and Mox-2 define a novel homeobox gene subfamily and are differentially expressed during early mesodermal patterning in mouse embryos, Development 116 (1992) 1123–1136. [PubMed: 1363541]

[31]. Boulet AM, Capecchi MR, Duplication of the Hoxd11 gene causes alterations in the axial and appendicular skeleton of the mouse, Dev Biol 249 (2002) 96–107. [PubMed: 12217321]

[32]. Lyons I, Parsons LM, Hartley L, Li R, Andrews JE, Robb L, Harvey RP, Myogenic and morphogenetic defects in the heart tubes of murine embryos lacking the homeo box gene Nkx2–5, Genes Dev 9 (1995) 1654–1666. [PubMed: 7628699]

[33]. Orii KE, Lee Y, Kondo N, McKinnon PJ, Selective utilization of nonhomologous end-joining and homologous recombination DNA repair pathways during nervous system development, Proc Natl Acad Sci U S A 103 (2006) 10017–10022. [PubMed: 16777961]

[34]. Nagaraju G, Hartlerode A, Kwok A, Chandramouly G, Scully R, XRCC2 and XRCC3 regulate the balance between short- and long-tract gene conversions between sister chromatids, Mol Cell Biol 29 (2009) 4283–4294. [PubMed: 19470754]

[35]. Snow MH, Gastrulation in the mouse: Growth and regionalization of the epiblast, J. Embryol. exp. Morph 42 (1977) 293–303.

[36]. Kafer GR, Cesare AJ, A Survey of Essential Genome Stability Genes Reveals That Replication Stress Mitigation Is Critical for Peri-Implantation Embryogenesis, Front Cell Dev Biol 8 (2020) 416. [PubMed: 32548123]

[37]. Berti M, Teloni F, Mijic S, Ursich S, Fuchs J, Palumbieri MD, Krietsch J, Schmid JA, Garcin EB, Gon S, Modesti M, Altmeyer M, Lopes M, Sequential role of RAD51 paralog complexes in replication fork remodeling and restart, Nat Commun 11 (2020) 3531. [PubMed: 32669601]

[38]. Somyajit K, Basavaraju S, Scully R, Nagaraju G, ATM- and ATR-mediated phosphorylation of XRCC3 regulates DNA double-strand break-induced checkpoint activation and repair, Mol Cell Biol 33 (2013) 1830–1844. [PubMed: 23438602]

[39]. Liu Y, Tarsounas M, O'Regan P, West SC, Role of RAD51C and XRCC3 in genetic recombination and DNA repair, J Biol Chem 282 (2007) 1973–1979. [PubMed: 17114795]

[40]. Garcin EB, Gon S, Sullivan MR, Brunette GJ, Cian A, Concordet JP, Giovannangeli C, Dirks WG, Eberth S, Bernstein KA, Prakash R, Jasin M, Modesti M, Differential Requirements for the RAD51 Paralogs in Genome Repair and Maintenance in Human Cells, PLoS Genet 15 (2019) e1008355. [PubMed: 31584931]

Highlights

- RAD51 paralog XRCC3 is required for mouse embryogenesis
- *Xrcc3* null embryos exhibit midgestational lethality
- *Trp53* loss prolongs embryo survival
- Mutation at a key ATPase residue also leads to embryonic lethality

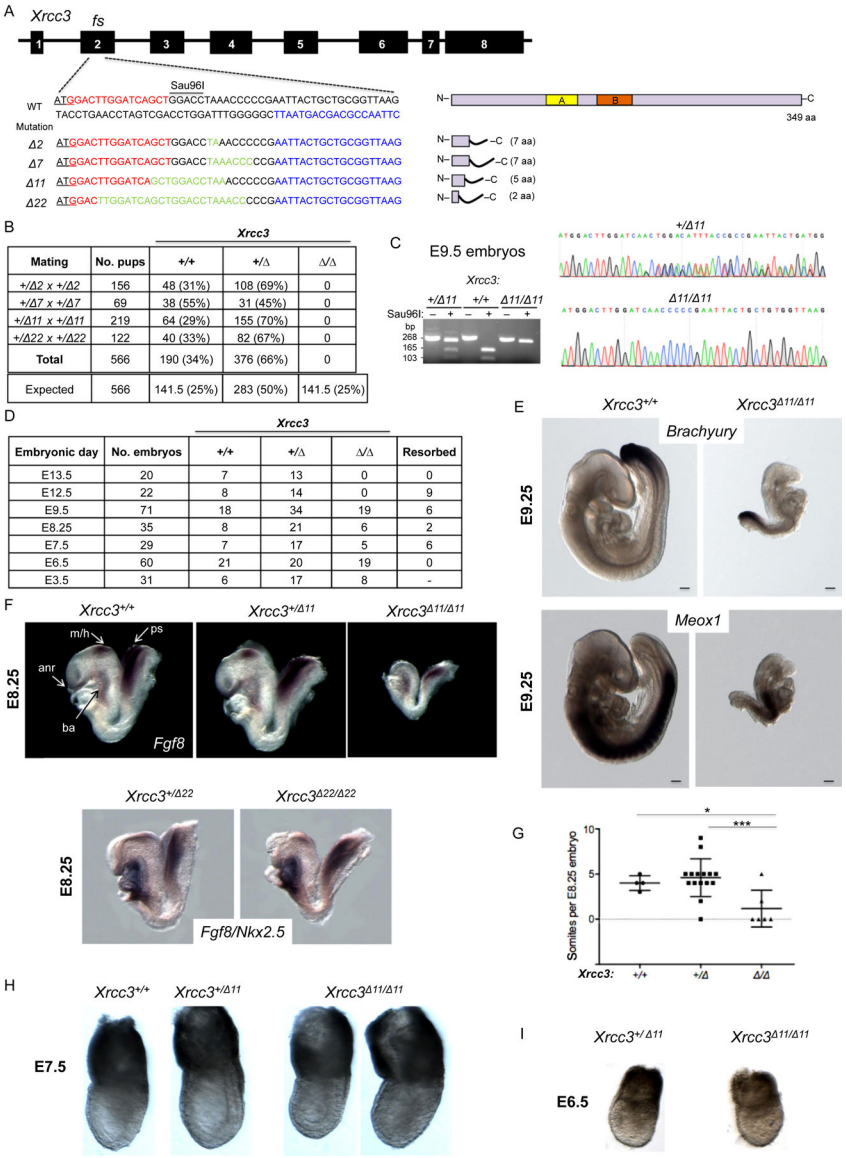

Mating	No. pups	+/+	+/Δ	Δ/Δ
+/Δ2 x +/Δ2	156	48 (31%)	108 (69%)	0
+/Δ7 x +/Δ7	69	38 (55%)	31 (45%)	0
+/Δ11 x +/Δ11	219	64 (29%)	155 (70%)	0
+/Δ22 x +/Δ22	122	40 (33%)	82 (67%)	0
Total	566	190 (34%)	376 (66%)	0
Expected	566	141.5 (25%)	283 (50%)	141.5 (25%)

Embryonic day	No. embryos	+/+	+/Δ	Δ/Δ	Resorbed
E13.5	20	7	13	0	0
E12.5	22	8	14	0	9
E9.5	71	18	34	19	6
E8.25	35	8	21	6	2
E7.5	29	7	17	5	6
E6.5	60	21	20	19	0
E3.5	31	6	17	8	-

Figure 1. *Xrcc3* is required during mouse development.

A. *Xrcc3* gene editing in mouse zygotes. TALENs were used to direct a double-strand break to exon 2, just downstream of the XRCC3 start codon (underlined). TALEN binding sequences are in red and blue. Mutations generated by injection of mouse zygotes with TALEN mRNA include small deletions (green) that result in frameshifts. The *Δ11* and *Δ22* alleles result in loss of a Sau96I restriction site that is useful for genotyping. Mouse XRCC3 is 349 amino acids with conserved Walker A and B boxes within an ATPase domain. Predicted protein truncations are indicated for each allele, showing the amount of coding sequence retained (2 to 7 amino acids) with tails of novel amino acids arising from the frameshift until the first stop codon.

B. *Xrcc3* mutant pups are not obtained at weaning for any of the four deletion alleles. Heterozygous animals are obtained at the expected Mendelian ratio if the homozygous mutants are not viable.

C. Genotyping of embryos obtained from timed matings at E9.5, verifying the presence of *Xrcc3*$^{\Delta 11/\Delta 11}$ embryos. The PCR amplicon of the *Δ11* allele is no longer cleavable by Sau96I. Sanger sequencing of the PCR product from the *Xrcc3*$^{\Delta 11/\Delta 11}$ embryos confirms the *Δ11* alleles.

D. *Xrcc3* mutant embryos are obtained at E9.5 and prior embryonic stages but not at E13.5.

E. *Xrcc3* mutant embryos at E9.5 are small and have not undergone turning to a fetal position (16 embryos unturned of 17 total). In situ hybridization for *Brachyury* labels the tail bud, while *Meox1* labels paraxial mesoderm which will form the somites.

F,G. *Xrcc3* mutant embryos at E8.25 appear grossly normal (**F**) but are developmentally delayed with fewer somites (**G**). In situ hybridization for *Fgf8* shows labeling of wild-type embryos at the midbrain/hindbrain boundary (m/h), the anterior neural ridge (anr), and the posterior end of the primitive streak (ps) while *Nkx2.5* labels the developing hear. Mutant embryos are variable for staining of the midbrain/hindgrain boundary.

H,I. *Xrcc3* mutant embryos at E7.5 (**H**) and E6.5 (**I**) appear grossly normal.

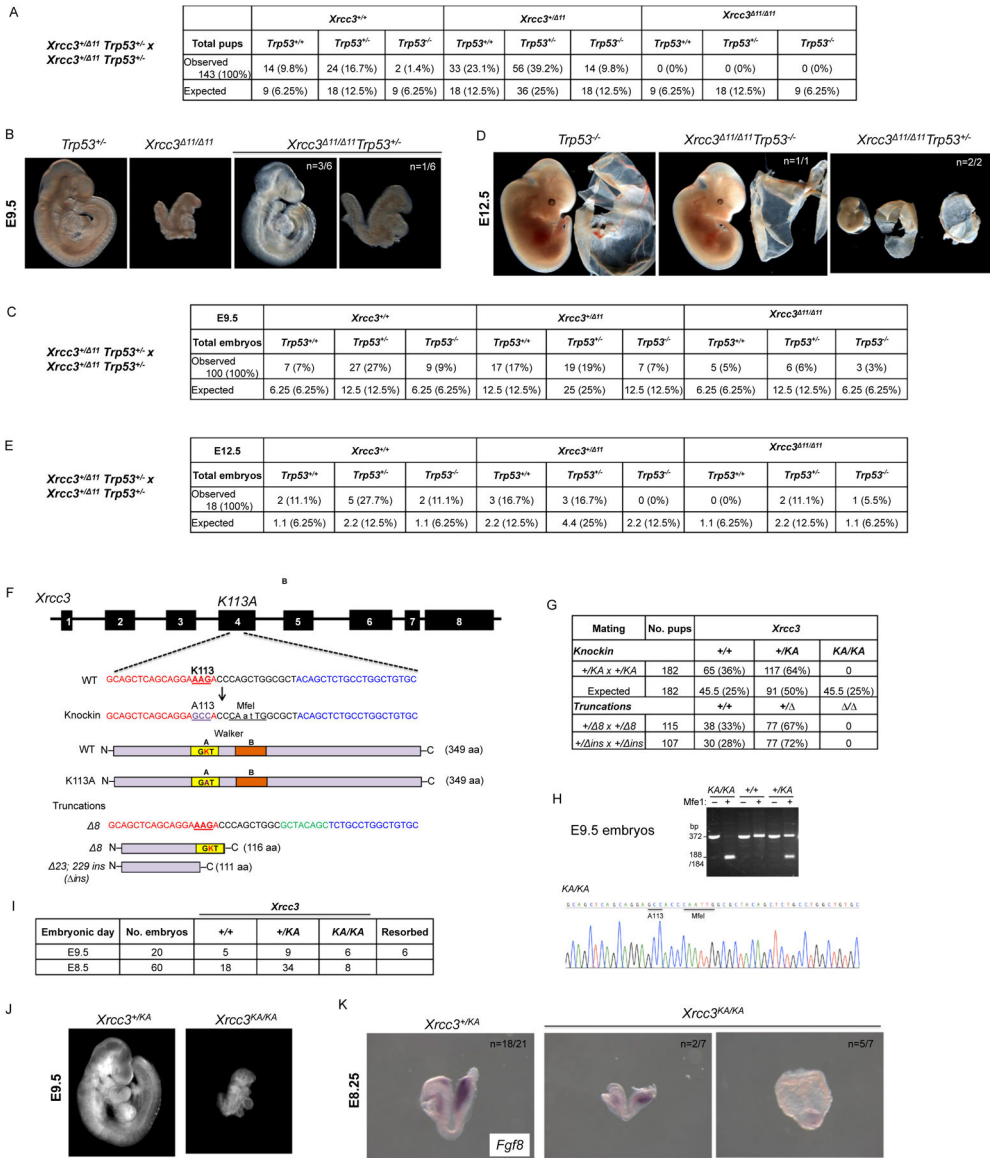

Figure 2. *Xrcc3* is required during mouse development.

A. *Xrcc3*$^{\Delta 11/\Delta 11}$ pups are not obtained at weaning even with homozygous or heterozygous mutation of *Trp53*.

B. Partial rescue of *Xrcc3* null phenotypes at E9.5 by concomitant *Trp53* mutation. Some *Xrcc3*$^{\Delta 11/\Delta 11}$ *Trp53*$^{+/-}$ embryos at E9.5 appear more like wild-type embryos (3 of 6 embryos), having turned to a fetal position, which was observed in only 1 of 17 *Xrcc3*$^{\Delta 11/\Delta 11}$ embryos without *Trp53* mutation. The other *Xrcc3*$^{\Delta 11/\Delta 11}$ *Trp53*$^{+/-}$ embryo that is shown has not turned and appears more like an *Xrcc3*$^{\Delta 11/\Delta 11}$ embryo. Of the remaining two *Xrcc3*$^{\Delta 11/\Delta 11}$ *Trp53*$^{+/-}$ embryos (Supplementary Figure 1), one is intermediate to these two phenotypes having partially turned, while the other appears developmental delayed.

C. Genotypes of E9.5 embryos obtained from *Xrcc3*$^{+/\Delta 11}$ *Trp53*$^{+/-}$ timed matings.

D. *Xrcc3*$^{\Delta 11/\Delta 11}$ *Trp53*$^{+/-}$ and *Xrcc3*$^{\Delta 11/\Delta 11}$ *Trp53*$^{-/-}$ embryos were observed at E12.5. The *Xrcc3*$^{\Delta 11/\Delta 11}$ *Trp53*$^{-/-}$ embryo appears reasonably normal, while the two *Xrcc3*$^{\Delta 11/\Delta 11}$ *Trp53*$^{+/-}$ embryos are runted although they have turned.

E. Genotypes of E12.5 embryos obtained from *Xrcc3*$^{+/\Delta 11}$ *Trp53*$^{+/-}$ timed matings.

F. *Xrcc3 KA* knockin mutation in the Walker A box using a 2 kb double-stranded DNA donor for homology-directed repair and a TALEN directed to exon 4. The donor contains the K113A mutation and two silent mutations (lower case) to create an MfeI restriction site for genotyping. In addition to the *KA* allele, two other alleles were established at the same time that contained out-of-frame mutations in exon 4 that are predicted to lead to truncations (*Δ8* and *Δ23;ins229*, which has an insertion derived from the donor plasmid for a net insertion of 206 bp).

G. *Xrcc3*$^{KA/KA}$ pups are not obtained at weaning. Homozygous mutants with truncations in exon 4 are also not obtained, as with truncations in exon 2.

H. Genotyping of embryos obtained from timed matings at E9.5, verifying the presence of *Xrcc3*$^{KA/KA}$ embryos. The PCR amplicon of the *KA* allele is cleavable by MfeI. Sanger sequencing of the PCR product from *Xrcc3*$^{KA/KA}$ embryos confirms the *KA* allele.

I. *Xrcc3*$^{KA/KA}$ embryos are obtained at E9.5 and E8.25.

J. *Xrcc3*$^{KA/KA}$ embryos at E9.25 are small and have not undergone turning to a fetal position.

K. *Xrcc3* mutant embryos at E8.25 can be grossly normal (2/7) or appear developmentally delayed (5/7).